RESEARCH

High expression of an unknown long noncoding RNA RP11-290L1.3 from GDM macrosomia and its effect on preadipocyte differentiation

Yu Lin[1],*, Yingying Zhang[1],*, Lei Xu[2],*, Wei Long[1], Chunjian Shan[1], Hongjuan Ding[1], Lianghui You[1], Chun Zhao[1] and **Zhonghua Shi[1]**

[1]State Key Laboratory of Reproductive Medicine, Women's Hospital of Nanjing Medical University, Nanjing Maternity and Child Health Care Hospital, Nanjing, People's Republic of China
[2]Maternal and Child Health Care Hospital of Dongchangfu District, Liaocheng, People's Republic of China

Correspondence should be addressed to C Zhao or Z Shi: zhaochun2008@yeah.net or jesse_1982@163.com

*(Y Lin, Y Zhang and L Xu contributed equally to this work)

Abstract

Aims: Gestational diabetes mellitus (GDM)-induced macrosomia is predominantly characterized by fat accumulation, which is closely related to adipocyte differentiation. An unknown long noncoding RNA RP11-290L1.3, referred to as RP11, was identified to be dramatically upregulated in the umbilical cord blood of women with GDM-induced macrosomia in our previous study. We conducted this study to identify the function of RP11 in GDM-induced macrosomia.
Methods: The effects of RP11 gain- and loss-of-function on HPA-v (human preadipocytes-visceral) adipogenesis were determined with lentivirus mediated cell transduction. The mRNA and protein expression levels of adipogenesis makers were evaluated by qPCR/Western blot. Then, we performed the microarray and pathway analysis to explore the possible mechanisms by which RP11 regulates adipogenesis.
Results: Overexpression of RP11 significantly enhanced adipocyte differentiation and increased the mRNA and protein expression levels of adipogenesis makers, such as PPARγ, SREBP1c, and FASN by qPCR/Western blot. Knockdown of RP11 showed opposite effects. Microarray and pathway analysis showed, after RP11 knockdown, 1612 genes were upregulated, and 583 genes were down-regulated which were found to be mainly involved in metabolic pathways, insulin signaling pathway and MAPK signaling pathway.
Conclusion: In conclusion, the unknown lncRNA RP11 serves as a positive factor on preadipocyte differentiation which could shed light on fetal fat accumulation in GDM.

Key Words
- ▶ long noncoding RNA
- ▶ GDM
- ▶ preadipocyte differentiation
- ▶ macrosomia
- ▶ fat accumulation

Introduction

Fetal overgrowth is the predominant adverse outcome of GDM. Fetal macrosomia, defined as growth beyond an absolute birth weight, typically 4000 g (1), is not only closely associated with high incidence of maternal complications, but also with increased susceptibility to obesity and type 2 diabetes in adults (2). GDM-induced macrosomia is mainly characterized by size increase of insulin-sensitive tissues and organs, especially the fat tissue (3, 4). Adipogenesis, during which preadipocytes develop into mature adipocytes, is a critical process for fat mass accumulation and obesity development. Although fetal hyperinsulinemia caused by maternal hyperglycemia has been considered as an important cause of GDM macrosomia, the precise pathogenesis by which GDM mother affects fetal fat accumulation though umbilical cord blood remains poorly understood.

Long noncoding RNAs (lncRNAs) are a class of endogenous RNA molecules with a length of more than 200 bases. Significant associations between altered lncRNA profiles and GDM-related complications, such as macrosomia or trophoblast dysfunction, have been observed (5). There is increasing evidence that lncRNAs play important roles in the physiological and pathological development of adipogenesis (6, 7), stem cell pluripotency (8), cancer (9), cell development and differentiation (10, 11), etc. Cui *et al.* (12) demonstrated that the transcribed ultraconserved lncRNA, uc.417, could serve as a negative regulator of brown adipose tissue thermogenesis through the p38 MAPK pathway. Recently, Sun *et al.* (6) identified 175 lncRNAs that are specifically regulated during adipogenesis. These lncRNAs were shown to be strongly involved in adipogenesis under the control of key transcription factors, such as peroxisome proliferator-activated receptor γ (PPARγ) and CCAAT/enhancer-binding protein α (C/EBPα).

With an aim to explore whether lncRNAs are involved in GDM-induced fat accumulation, we hybridized the umbilical cord vein blood from normal pregnancy and GDM-induced macrosomia groups to a microarray. The results were deposited in NCBI's Gene Expression Omnibus (accession number GSE65737) (http://www.ncbi.nlm.nih.gov/geo/query/acc.cgi?acc=GSE65737) (13). Of the 1151 differentially expressed lncRNAs, the expression of lncRNA RP11-290L1.3 (RP11; ENST00000552367) was identified to be dramatically upregulated in the umbilical cord blood of women with GDM-induced macrosomia (fold change of 14.1039315); however, its function remains unknown.

In this study, we analyzed the clinical correlation between the expression of RP11 in the umbilical cord blood and neonatal fat mass (FM), F% (percent of body fat), and neonatal birth weight. The role of RP11 in adipogenesis was investigated by performing knockdown and overexpression experiments in human preadipocytes-visceral (HPA-v). Furthermore, the possible mechanisms by which RP11 regulates adipogenesis were primarily explored by microarray analysis of RP11-silenced HPA-v.

Materials and methods

Ethics statement

This study was conducted in accordance with the Declaration of Helsinki and was approved by the Ethics Committee of the Women's Hospital of Nanjing Medical University. Written informed consent was obtained from all subjects prior to enrolment.

Subjects

All subjects enroled in this study attended regular prenatal check-ups and delivered their babies at the Women's Hospital of Nanjing Medical University in 2017. GDM was diagnosed using a standardized 75 g oral glucose tolerance test (OGTT) at 24–28 weeks of pregnancy. Based on the International Association of Diabetes and Pregnancy Study Group criteria (14), GDM was diagnosed if one or more of the following abnormality were met: glucose level equal to or greater than fasting 5.1 mmol/L, 1-h post load 10.0 mmol/L, or 2-h post load 8.5 mmol/L. Strict diet and exercise control or insulin treatment was administrated to achieve the goal of fasting glucose level of less than 5.3 mmol/L and 2-h postprandial level of less than 6.7 mmol/L.

The exclusion criteria for mothers were as follows: multiple pregnancies, hypertensive disorders, history of diabetes prior to conception, polycystic ovary syndrome, Cushing's syndrome, pheochromocytoma, acromegaly, history of smoking, chemical dependency, use of assisted reproductive technology, multiple gestation, and any other confounding pathologies, including hyperthyroidism and hypothyroidism. The exclusion criteria for infants were as follows: preterm birth, fetal growth restriction, fetal congenital anomalies, and other confounding pathologies, such as neonatal infection. In this study, 32 GDM subjects with neonatal birth weights equal to or exceeding 4 kg (macrosomia group) and 47 non-GDM controls with neonatal birth weights less than 4 kg (control group) were enrolled. Both maternal and neonatal characteristics are presented in Table 1.

Sample collection

Umbilical cord blood samples from the macrosomia and control groups were collected at the time of cesarean or vaginal delivery. Whole blood was separated into serum and cellular fractions by centrifugation at 1574 ***g*** for 10 min, followed by centrifugation at 14,167 ***g*** for 15 min to completely remove any cell debris. The plasma sample (2 mL) from each woman was filtered through a 0.22 μm filter (MILLEXGV; Millipore) and then mixed with 2 mL TRIzol reagent and 0.4 mL chloroform. Following this, the aqueous layer was transferred to a new tube and 1.5 mL of 70% ethanol was added. This mixture was then applied on the RNeasy mini column (Qiagen) according to the manufacturer's recommendations. RNA quantity and quality were measured using the NanoDrop ND-1000 spectrophotometer. Total RNA was eluted with

Endocrine CONNECTIONS

Table 1 Maternal and neonatal characteristics of control group and GDM group.

	Control group (*n* = 47)	**GDM** (*n* = 32)	***P* value**
Maternal characteristics			
Age (years)	28.1 ± 0.85	28.0 ± 2.70	0.85
Gravidity	1.43 ± 0.74	1.69 ± 0.85	0.17
Parity	1.17 ± 0.38	1.22 ± 0.42	0.60
Pre-pregnancy BMI (kg/m^2)	23.2 ± 1.80	22.2 ± 1.85	0.02
HbA1C (%)	5.31 ± 0.64	5.40 ± 0.59	0.52
OGTT, fasting (mmol/L)	4.68 ± 0.38	4.93 ± 0.38	0.01
OGTT, 1 h (mmol/L)	9.11 ± 0.56	9.82 ± 0.62	3.3E-06
OGTT, 2 h (mmol/L)	7.74 ± 0.53	8.12 ± 0.52	0.003
Gestational week	39.3 ± 0.83	39.3 ± 0.54	0.70
Delivery mode (vaginal delivery)	35 (47.5%)	18 (56.3%)	0.15
Triglycerides (mmol/L)	3.89 ± 1.25	4.72 ± 1.71	0.03
Cholesterol (mmo/L)	6.94 ± 1.47	7.66 ± 1.53	0.04
Insulin therapy	0 (0%)	6 (18.8%)	
Neonatal characteristics			
Birth weight (kg)	3.40 ± 0.31	4.20 ± 0.11	1.7E-23
Gender (male)	29 (61.7%)	19 (59.4%)	1.00
Bicipital (mm)	3.9 ± 0.3	4.0 ± 0.3	0.26
Tricipital (mm)	5.8 ± 1.4	7.6 ± 0.4	8E-11
Subscapular (mm)	5.7 ± 0.3	7.5 ± 0.4	3.4E-31
Skinfold thicknesses (mm)	5.8 ± 0.3	7.5 ± 0.3	4.87E-35
Neonatal body fat mass (FM) (g)	648 ± 111	960 ± 52.3	7E-26
Fat percentage (F%)	18.9 ± 1.60	22.9 ± 0.68	5.4273E-23
SFT4 (mm)	21.2 ± 2.01	26.5 ± 1.03	2.83E-24
Body density (D)	1.03 ± 0.002	1.02 ± 0.001	6.7E-23

SFT4 equals to the sum of bicipital, tricipital, subscapular, and suprailiacal skinfold thicknesses; body density (D) = 1.1235-0.0719 × log (SFT4); FM = F% × body weight; F% = (585/D-550) × 100%.

20 μL RNase-free water after DNase digestion and then stored in liquid nitrogen (15).

Neonatal body composition analysis

Anthropometric measurements, including bicipital, tricipital, subscapular, and suprailiacal skinfold thicknesses were performed for 79 infants within 12 h after childbirth. All measurements were performed by a well-trained neonatologist. Each measurement was repeated three times, and the results were averaged. Neonatal body FM and fat percentage (F%) were calculated according to the Weststrate method (16), as follows: SFT4 = the sum of bicipital, tricipital, subscapular, and suprailiacal skinfold thickness; body density (D) = 1.1235-0.0719 × log(SFT4); F% = (585/D-550) × 100%; FM = F% × body weight. The neonatal characteristics are presented in Table 1.

Quantitative reverse transcription polymerase chain reaction (qRT-PCR)

Total RNA was isolated using TRIzol reagent (Invitrogen) and then reverse transcribed using the PrimeScript® RT reagent kit with gDNA Eraser (Perfect Real Time) (Takara)

according to the manufacturer's instructions. The expression of RP11 in the blood samples and HPA-v cells was measured by qRT-PCR. Glyceraldehyde 3-phosphate dehydrogenase (GAPDH) was used as the internal control. The RP11 primer sequences used were as follows: sense, TTCAGGCAGAGTTGGAGGTG and antisense, GGCAAGGAGATCGACTTTCG. The relative expression of RP11 was determined using the $2^{-\Delta\Delta Ct}$ method and normalized to GAPDH expression. Information on the primers used is presented in Table 2.

Cell culture and preadipocyte differentiation

HPA-v (ScienCell Research Laboratories, San Diego, CA, USA) were cultured in preadipocyte medium (PAM; ScienCell Research Laboratories) supplemented with 5% fetal bovine serum (Gibco), 1% preadipocyte growth supplement (ScienCell Research Laboratories), and 1% penicillin/streptomycin at 37°C in 5% CO_2.

To induce differentiation, confluent HPA-v (day 0) were cultured in differentiation medium containing serum-free PAM supplemented with 250 nM insulin, 1 mM dexamethasone, 0.5 mM 3-isobutyl-1-methylxanthine, and 1 μM rosiglitazone. The culture medium was

Table 2   Primers qRT-PCR.

Gene	Forward primer	Reverse primer
RP11-290L1.3	TTCAGGCAGAGTTGGAGGTG	GGCAAGGAGATCGACTTTCG
PPAR-γ	AGCCTGCGAAAGCCTTTTGGTG	GGCTTCACATTCAGCAAACCTGG
FABP4	ACGAGAGGATGATAAACTGGTGG	GCGAACTTCAGTCCAGGTCAAC
FASN	TTCTACGGCTCCACGCTCTTCC	GAAGAGTCTTCGTCAGCCAGGA
LPL	CTGCTGGCATTGCAGGAAGTCT	CATCAGGAGAAAGACGACTCGG
C/EBP-alpha	AGGAGGATGAAGCCAAGCAGCT	AGTGCGCGATCTGGAACTGCAG
GLUT4	CCATCCTGATGACTGTGGCTCT	GCCACGATGAACCAAGGAATGG
SREBP-1c	ACTTCTGGAGGCATCGCAAGCA	AGGTTCCAGAGGAGGCTACAAG

replaced after 4 days. Cells were then cultured in serum-free Dulbecco's modified Eagle's medium containing 250 nM insulin, which was replaced every 2 days until lipid accumulation was observed in the cells (day 10). HPA-v were harvested on days 0, 1, 4, 8, and 10 for further experiments.

Lentivirus-mediated overexpression of lncRNA RP11

The viral vector we used contains an open reading frame for GFP. lncRNA RP11 was overexpressed in HPA-v using recombinant lentiviral vectors (GenePharma Co., Ltd, Shanghai, China) containing either pre-lncRNA RP11 or negative control precursor lncRNA. For lentiviral infection, preadipocytes were plated overnight in 6-well plates (Corning) at a concentration of 3×10^5 cells per well. On reaching about 40% confluency, the stage at which the transfection efficiency is optimal, preadipocytes were transfected with either lncRNA RP11 overexpression lentiviral vector or negative control in 5 μg/mL polybrene (Sigma–Aldrich). At 24 h post transfection, fresh medium was added to the preadipocyte culture. Green fluorescent protein (GFP) levels were measured at 48 and 72 h post transfection, and the expression of lncRNA RP11 was verified using qRT-PCR. After the transfected cells reached confluency, differentiation was induced as described previously.

Lentivirus-mediated knockdown of lncRNA RP11

lncRNA RP11 was knocked down in HPA-v using recombinant lentiviral vectors (GenePharma Co., Ltd, Shanghai, China) containing either negative control precursor lncRNA and two anti-lncRNAs against lncRNA RP11 (SH1 and SH2). The sequences of SH1 and SH2 were as follows: ACCGAAAGTCGATCTCCTTGC and GTGCAGTTCCTTGAGCTTGAC, respectively.

For lentiviral infection, preadipocytes were processed as described previously. The lentivirus-mediated expression of lncRNA RP11 was verified using qRT-PCR.

Oil red O staining

In vitro differentiated cells (day 8) were washed with PBS, followed by fixation with 4% paraformaldehyde for 30 min at room temperature. Next, cells were washed twice with 60% isopropanol and stained with 0.6% (w/v) filtered oil red O solution (Sigma–Aldrich; stock solution, 3 mg/mL in isopropanol; working solution, 60% oil red O stock solution and 40% distilled water) for 30 min at 37°C. Cells were then washed with PBS to remove an unbound dye, and visualized and photographed under a microscope (Axio–Home; Carl Zeiss) at ×200 magnification. The intracellular triglyceride content relative to total protein content was measured using the Triglyceride Assay kit (Applygen Technologies Inc., Beijing, China) and BCA Protein Assay kit (Pierce) according to the manufacturer's instructions. At the indicated time points, mature adipocytes were treated with lysis buffer, and the cell lysates were harvested and homogenized. Subsequently, the cell suspension was retained to detect the triglyceride and protein concentrations.

Proliferation assay

Cell proliferation assay was performed using the CellTrace™ Far Red Cell Proliferation kit (Invitrogen) for flow cytometry. Briefly, human preadipocytes were first transfected with either the lncRNA RP11 overexpression/knockdown or negative control lentiviral vector. At 48 h post transfection, isolated cells were plated in 6-well plates at a density of 1×10^5 cells per well, until they reached 50% confluency. CellTrace™ medium was added to each well of the plate according to the manufacturer's instructions. Next, the dyed cells were cultured for 1 h at

37°C, and then imaged and counted by flow cytometry (MoFlo XDP; Beckman Coulter, USA) at a 72 h time point. The cell proliferation assay was performed independently for three times.

Western blotting

Cells were lysed in lysis buffer containing 20 mM Tris–HCl (pH 8.0), 150 mM NaCl, 10% glycerol, 20 mM beta-glycerol phosphate, 1% NP-40, 5 mM EDTA, and 0.5 mM EGTA supplemented with protease inhibitors (Roche Applied Science). The cell extracts were boiled in sodium dodecyl sulfate (SDS) loading buffer (150 mM Tris–HCl (pH 6.8), 12% SDS, 30% glycerol, 0.02% bromophenol blue, and 6% 2-mercaptoethanol) at 95°C for 10 min. Protein content was measured using the Pierce BCA Protein Assay kit (Thermo Fisher Scientific), according to the manufacturer's instructions. Next, proteins (30 g) were separated on 10% SDS-polyacrylamide gels and transferred to a 0.2 μm PVDF membrane (Millipore). After blocking with 5% skimmed milk, the membranes were incubated overnight at 4°C with appropriate primary antibodies against SREBP1c (Abcam), peroxisome proliferator-activated receptor gamma (PPARγ; Abcam), C/EBPα (Abcam), FABP4 (Abcam), LPL (Abcam), FASN (Abcam), and GAPDH (Abcam). Subsequently, the membranes were hybridized with a secondary antibody conjugated with peroxidase (Santa Cruz Biotechnology). The protein levels were quantitated using the ChemiDoc system (Bio–Rad).

Microarray analysis

lncRNA RP11 expression was knocked down in HPA-v using anti-lncRNA against lncRNA RP11 (SH1 and SH2). After differentiation was induced as previously described, total RNA was isolated from differentiated cells using an RNeasy kit (Qiagen). After RNA quality determination and RT, microarray analysis for detection of gene expression was performed using a Whole Human Genome Microarray (Agilent Technologies) according to the manufacturer's protocol. Data were extracted using the Agilent Feature Extraction software (version 9.5). Differentially expressed genes between the SH1/SH2 and control groups were identified, and an intersection was made. Differentially intersecting genes were identified via analyzing the fold change and the Student's *t*-test *P* value. For fold change analysis, a cutoff value of 2 was used. Next, all candidate genes were mapped to gene ontology (GO) terms in the database (http://www.geneontology.org/).

Pathway analysis is a functional analysis that maps genes to the Kyoto Encyclopedia of Genes and Genomes (KEGG; http://www.genome.jp/kegg) pathways.

Statistical analysis

Means and standard deviations were calculated for demographic data. The differential expression of RP11 between normal control and GDM women complicated with macrosomia was analyzed by Student's *t*-test using SPSS software (version 17.0; SPSS). $P < 0.05$ was considered statistically significant.

Pearson's correlation coefficient analysis was used to analyze the correlation between the relative expression of RP11 (normalized to GAPDH) and neonatal birth weight, F%, or FM in the umbilical cord blood of 79 subjects. $P < 0.05$ was considered statistically significant.

Results

RP11 is a highly conserved lncRNA

lncRNA RP11 is an intergenic lncRNA located on chromosome 12q21.2 in the human genome. Multiple alignment analysis of the RP11 locus showed that it is highly conserved in the rhesus, human, mouse, dog, and elephant genomes using the University of California Santa Cruz (UCSC) genome browser (Santa Cruz; http://genome.ucsc.edu). The RP11 sequence in the human and mouse genomes showed 81.37% identity.

Maternal and neonatal demographic and anthropometric parameters

Analysis of maternal and neonatal demographic and anthropometric characteristics showed that there were no significant differences in maternal age, gestational age, gravidity, parity, nulliparous and neonatal gender between the GDM macrosomia and normal control groups ($P > 0.05$). However, the pre-pregnancy BMI and OGTT results of women in the macrosomia group were higher than that of women in the control group ($P < 0.05$), and the neonatal anthropometric parameters, including birth weight, tricipital SF, subscapular SF, suprailiacal SF, SFT4, neonatal body FM, and F%, but excluding bicipital SF were dramatically higher in the macrosomia group ($P < 0.01$; Table 1).

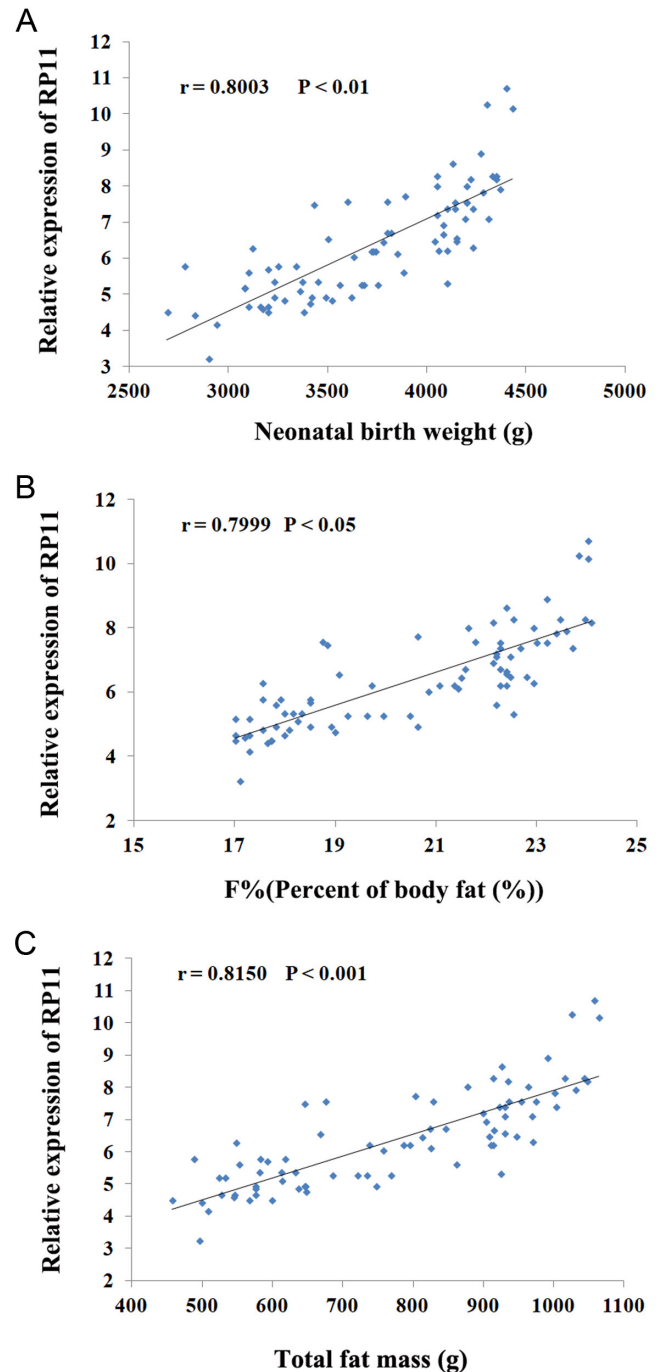## Correlation between RP11 expression and neonatal body composition

Pearson's correlation coefficient analysis suggested a significant positive correlation between RP11 expression and neonatal birth weight (r=0.8003, $P < 0.01$), F% (r=0.7999, $P < 0.05$) and FM (r=0.8150, $P < 0.001$) (Fig. 1).

Effect of RP11 overexpression on preadipocyte proliferation and differentiation

RP11 was overexpressed in HPA-v using recombinant lentiviral vectors containing pre-RP11 and negative control precursor. The preadipocytes did not show significant morphological changes after RP11 overexpression (Fig. 2A). qRT-PCR results confirmed that RP11 was significantly overexpressed in the RP11 overexpression group compared to the control group ($P < 0.001$; Fig. 2B). Results of cell proliferation assay showed that human preadipocytes transfected with RP11 overexpression or negative control lentivirus exhibited proliferation rates of 50.6 and 46.8%, respectively. There was no significant difference in proliferation rate between the two groups ($P > 0.05$; Fig. 2E). Differentiation of human preadipocytes stably transfected with RP11 overexpression or negative control lentivirus was then induced. Measurement of the triacylglycerol content showed that lipid accumulation was significantly increased in RP11-overexpressing cells on day 7 of adipogenesis (Fig. 3A). The morphology of the cells and the size of the lipid droplets were analyzed by oil red O staining. More than 80% of the cells in the control group had differentiated into mature adipocytes, and lipid droplets accumulation was more obvious after RP11 overexpression (Fig. 3B). Subsequently, the effects of RP11 overexpression on several important factors involved in the differentiation of preadipocytes were evaluated. Results showed that the mRNA and protein expression levels of PPARγ, SREBP1c, and FASN were dramatically increased in the RP11 overexpression group, whereas those of LPL and C/EBPEα were not significantly altered (Fig. 3C and D).

Effect of RP11 silencing on preadipocyte proliferation and differentiation

RP11 expression was silenced in HPA-v using two lentiviral vectors: SH1 (ACCGAAAGTCGATCTCCTTGC) and SH2 (GTGCAGTTCCTTGAGCTTGAC). The preadipocytes did not show significant morphological changes after RP11 silencing (Fig. 2C). qRT-PCR results confirmed that
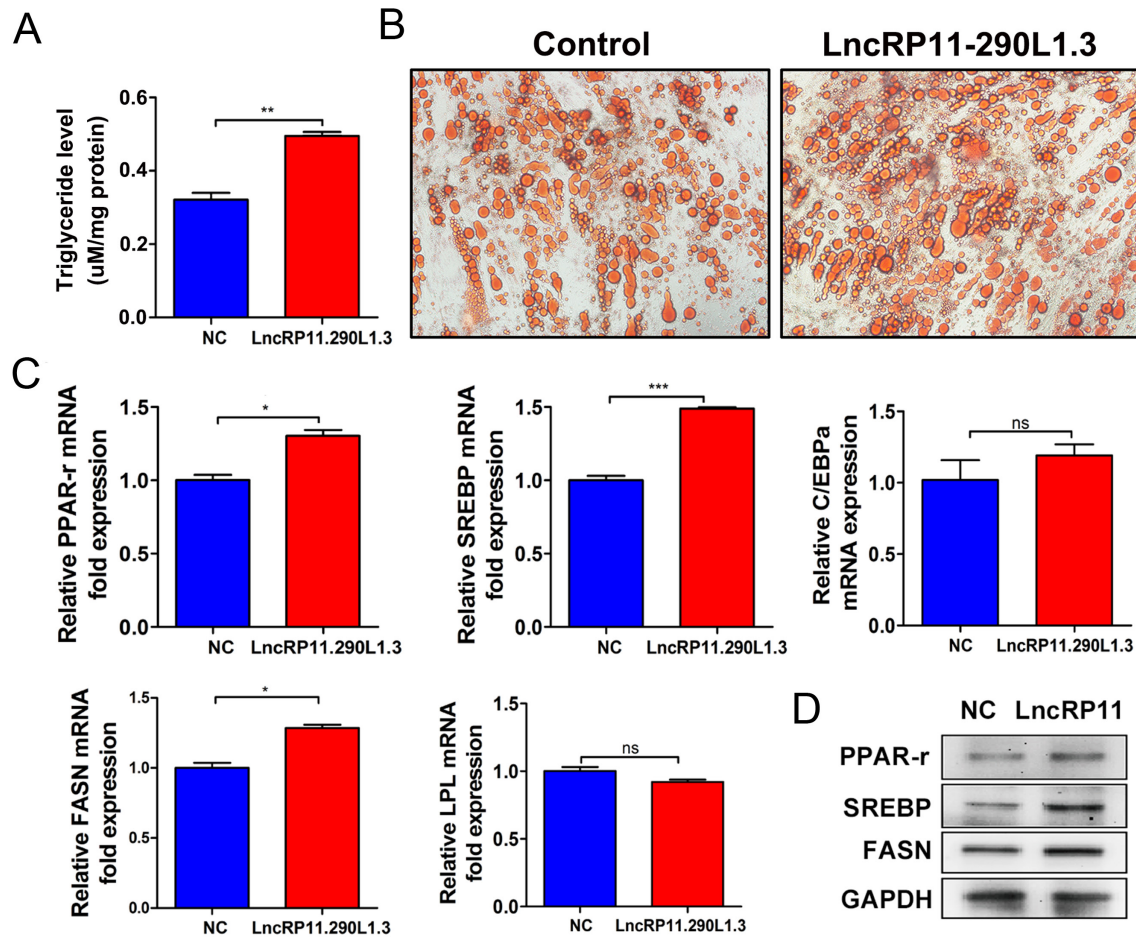

Figure 1
Strong positive correlation between relative expression of RP11 (GAPDH normalized) and neonatal birth weight (A), percent of body fat (B) or fat mass (C) in umbilical cord blood by Pearson's coefficient correlation analysis.

RP11 expression was dramatically down-regulated in the SH1 and SH2 groups compared with the control group (Fig. 2D). SH1 ($P < 0.01$) and SH2 ($P < 0.001$) lentiviral vectors were chosen for further experiments. Results of cell proliferation assay indicated that preadipocyte
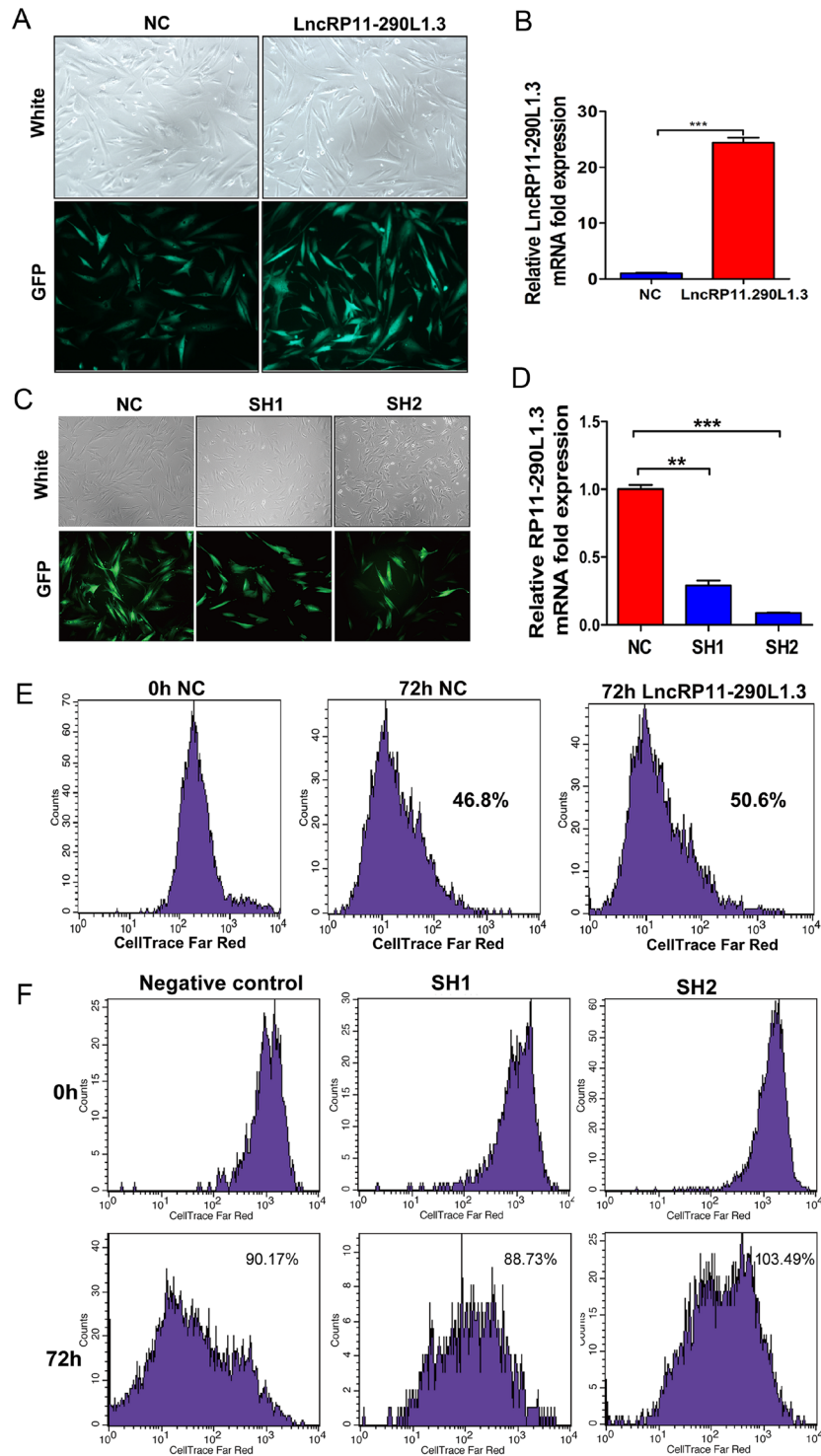
Figure 2

Effects of RP11 overexpression or silence on preadipocyte proliferation by flow cytometry. Fluorescence microscopy to detect preadipocytes morphology changes after RP11overexpression (A) or silence (C). (B) The preadipocytes did not show significant morphological changes in all groups. The relative expression of RP11 normalized to GAPDH expression in control and RP11 overexpression groups. (D) The relative expression of RP11 normalized to GAPDH expression in control and RP11 silence groups. RP11 was dramatically down-regulated in SH1 ($P < 0.01$) and SH2 ($P < 0.001$) group. (E) Effects of RP11 overexpression on preadipocyte proliferation by flow cytometry ($P < 0.001$). Left: 0 h in negative control group. Middle: 72 h incubation after RP11 overexpression in negative control. Right: 72 h incubation after RP11 overexpression in RP11 overexpression group ($P > 0.05$). (F) Effects of RP11 silence on preadipocyte proliferation by flow cytometry. Left: 0 h in negative control group. Middle: 72 h incubation after RP11 silence by SH1 ($P > 0.05$). Right: 72 h incubation after RP11 silence by SH2 ($P > 0.05$).

Figure 3
Effects of RP11 overexpression on preadipocyte differentiation. (A) Triacylglycerol content detected lipid accumulation at day 7 during adipogenesis ($P < 0.01$). (B) Intracellular lipid accumulation during differentiation stained with oil red. The results showed more fat droplets accumulation after RP11 overexpression ($P < 0.05$). (C) mRNA expressions of five important factors involved in preadipocytes differentiation. The results showed that mRNA expressions of PPARγ ($P < 0.01$), SREBP1c ($P < 0.001$) and FASN ($P < 0.05$) were significantly increased in RP11 overexpression group, whereas the expressions of LPL and C/EBPEα were not obviously changed ($P > 0.05$). (D) Protein expressions of three important factors involved in preadipocytes differentiation. The results showed that protein expressions of PPARγ ($P < 0.05$), SREBP1c ($P < 0.001$) and FASN ($P < 0.05$) were significantly increased in RP11 overexpression group.

proliferation was not significantly altered after RP11 silencing ($P > 0.05$; Fig. 2F).

Measurement of the triacylglycerol content showed that lipid accumulation was significantly decreased in the SH1 and SH2 groups on day 7 of adipogenesis (Fig. 4A). Oil red O staining results for intracellular lipid accumulation during differentiation showed significantly less fat droplet accumulation after RP11 silencing (SH1: $P < 0.001$, SH2: $P < 0.001$) (Fig. 4B). Further, our results showed that the mRNA expression of PPARγ (SH1: $P < 0.001$, SH2: $P < 0.001$), SREBP1c (SH1: $P < 0.05$, SH2: $P < 0.01$), FASN (SH1: $P < 0.01$, SH2: $P < 0.001$), and LPL (SH1: $P < 0.001$, SH2: $P < 0.001$) was significantly decreased in the RP11-silenced groups, while that of C/EBPEα was not significantly altered ($P > 0.05$) (Fig. 4C). The protein expression of the four important

factors involved in preadipocyte differentiation was then analyzed. The results showed that the protein expression of PPARγ (SH1: $P < 0.001$, SH2: $P < 0.001$), SREBP1c (SH1: $P < 0.001$, SH2: $P < 0.05$), FASN (SH1: $P < 0.001$, SH2: $P < 0.01$), and LPL (SH1: $P > 0.05$, SH2: $P < 0.05$) was significantly decreased after RP11 silencing (Fig. 4D).

Differentially expressed mRNAs after RP11 silencing

lncRNAs can modulate expression of genes that are positioned in the vicinity of their transcription sites in a *cis*-acting manner (17). To identify molecular mediator response to RP11, we used a transcription position bioinformatic anaylsis and found RP11 sites located
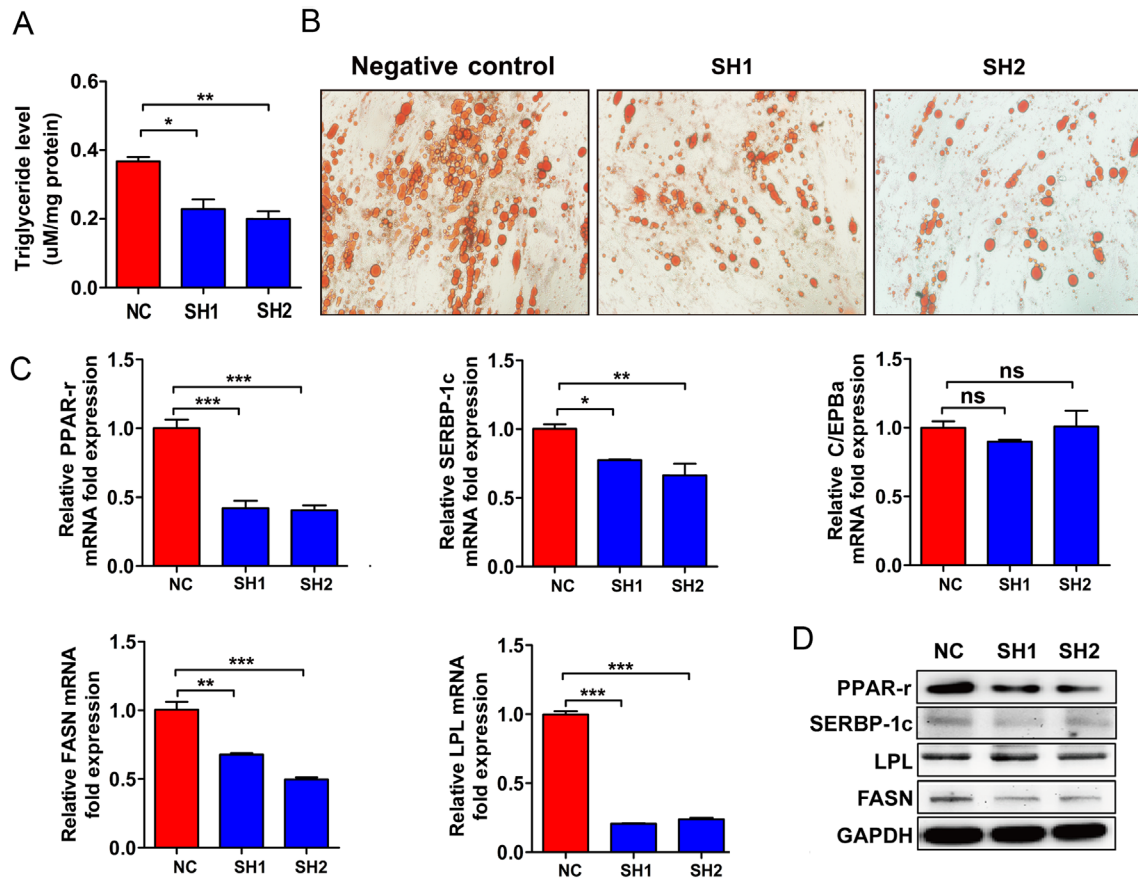
Figure 4

Efficiency of RP11 silence in preadipocyte. (A) Triacylglycerol content detected lipid accumulation at day 7 during adipogenesis (SH1: $P < 0.05$, SH2: $P < 0.01$). (B) Intracellular lipid accumulation during differentiation stained with oil red. The results showed significantly less fat droplets accumulation after RP11 silence (SH1: $P < 0.001$, SH2: $P < 0.001$). (C) mRNA expressions of five important factors involved in preadipocytes differentiation. The results showed that mRNA expressions of PPARγ (SH1: $P < 0.001$, SH2: $P < 0.001$), SREBP1c (SH1: $P < 0.05$, SH2: $P < 0.01$), FASN (SH1: $P < 0.01$, SH2: $P < 0.001$) and LPL (SH1: $P < 0.001$, SH2: $P < 0.001$) were significantly decreased in RP11 silence groups, whereas the expressions of C/EBPEα were not obviously changed ($P > 0.05$). (D) Protein expressions of four important factors involved in preadipocytes differentiation. The results showed that protein expressions of PPARγ (SH1: $P < 0.001$, SH2: $P < 0.001$), SREBP1c (SH1: $P < 0.001$, SH2: $P < 0.05$), FASN (SH1: $P < 0.001$, SH2: $P < 0.01$) and LPL (SH1: $P > 0.05$, SH2: $P < 0.05$) were significantly decreased after RP11 was silenced.
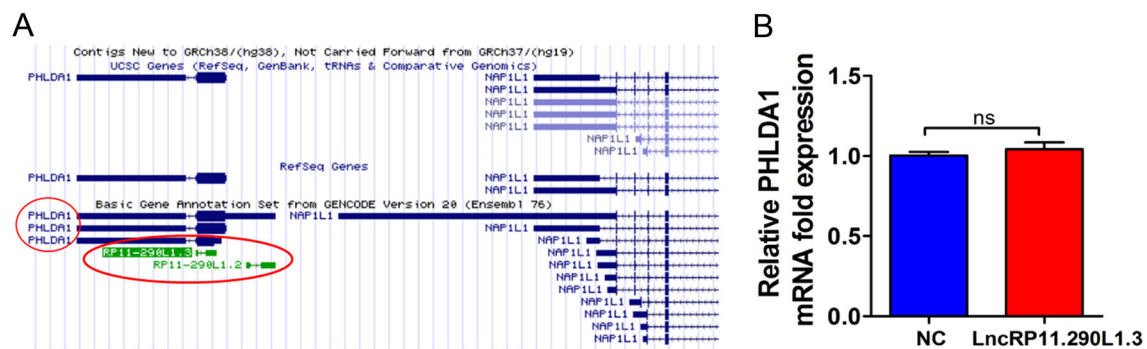
Figure 5

Study on the relationship between RP11 and PHLDA1. (A) The transcriptional position analysis of RP11 in the mouse genome. PHLDA1 is located upstream of RP11. (B) The transcriptional of PHLDA1 was unaffected by RP11 overexpression.

within pleckstrin homology-like domain, family A, member 1 (PHLDA1) (Fig. 5A). We also examined the expression of PHLDA1 in RP11-overexpressed adipocytes. However, the expression of PHLDA1 was unaffected (Fig. 5B), providing the evidence that RP11 does not act in *cis* to regulate expression of its neighbor.

To further understand the mechanism by which RP11 regulates the adipocyte thermogenic program, we performed gene chip analysis of differentiated RP11 silenced adipocytes. RP11 expression was silenced by transfection with the SH1 or SH2 lentiviral vector. Using microarray analysis, a total of 4765 differentially expressed mRNAs were identified between the SH1 and control groups, and a total of 3833 mRNAs were identified between the SH2 and control groups (fold change ≥ 2, $P < 0.05$). Intersection analysis showed that 1612 genes were upregulated in both the SH1 and SH2 groups as compared with the control group, whereas 583 genes were down-regulated in both the SH1 and SH2 groups (Fig. 6A and B). The top 20 up- and down-regulated mRNAs between the RP11-silenced and control groups are presented in Table 3.

GO and pathway analysis

Intersection of differentially expressed genes was analyzed by GO and pathway analyses to determine the genes attributes in biological process, cellular components, and molecular functions (Supplementary Figures 1 and 2, see section on supplementary materials given at the end of this article). Among them, 1612 upregulated genes were found to be involved in cytokine–cytokine receptor interaction, sphingolipid metabolism, NOD-like receptor signaling pathway, etc. Interestingly, 583 down-regulated genes were found to be involved in metabolic pathways, insulin signaling pathway, and triglyceride metabolic process, which have been reported to be closely related with preadipocyte differentiation (Fig. 6C and D).

Discussion

GDM is a common disease during pregnancy, which may lead to fetal metabolic disorders, such as macrosomia, hyperglycemia, diabetes, obesity, and cardiovascular disease (18). GDM-induced macrosomia also can cause shoulder dystocia, postpartum hemorrhage, and an increase in the rate of cesarean sections. As mentioned previously, adipogenesis is a critical process involved in fat accumulation and obesity development, and RP11 is

highly expressed in the umbilical cord blood of women with GDM-induced macrosomia, suggesting the need to further explore the association between RP11 and GDM-induced fat accumulation.

According to our research, we found that RP11 expression may be an important factor that regulates neonatal body FM and fat percentage. Following RP11 overexpression, more number of lipid droplets were accumulated in the cells, indicating the more active process of lipid uptake and TG synthesis. Moreover, the expression of certain crucial transcription factors, like PPARγ was obviously increased in the RP11 overexpression group, which was consistent with the results of oil red O staining. Basseri *et al.* (19) demonstrated that loss of PHLDA1 results in mature-onset obesity and insulin resistance by regulating lipogenesis. We also examined the expression of PHLDA1 in RP11-overexpressed adipocytes. However, the expression of PHLDA1 was unaffected. Furthermore, RP11 silencing decreased preadipocyte differentiation. For a comprehensive understanding of RP11 function, we performed microarray analysis after RP11 silencing, and found that the differ or upregulated downstream genes were enriched in some biological processes related to interferon (IFN) responses, type I IFN signaling, and IFN-inducing pathways, such as the TLR pathway, while the down-regulated downstream genes were involved in triglyceride metabolic process, energy reserve metabolic process, insulin signaling pathway, MAPK signaling, and other processes.

It is well known that obesity is caused due to an imbalance between food intake and energy consumption. Because of extra nutrient uptake, excess fatty acids and glucose are used to be the substrates of the synthesis for triglyceride in adipocytes, which eventually results in obesity (20). Fat accumulation is determined by the balance between triglyceride synthesis and breakdown. After the uptake of carbohydrates, the circulating glucose is taken up by adipocytes and converted into pyruvate through glycolysis. Pyruvate oxidation plays a vital role in the tricarboxylic acid (TCA) cycle. Citrate, an intermediate in the TCA cycle, is an important substrate for *de novo* lipogenesis (21). Results of microarray analysis showed that pathways associated with pyruvate metabolism and TCA cycle were down-regulated, meaning that the *de novo* lipogenesis is suppressed, which in turn leads to the decrease of fat deposition. Thus we can suppose that dysfunction of metabolic pathways contributes to the development of obesity.

The insulin signaling pathway also plays a critical role in glucose and lipid metabolism. Normally, secreted
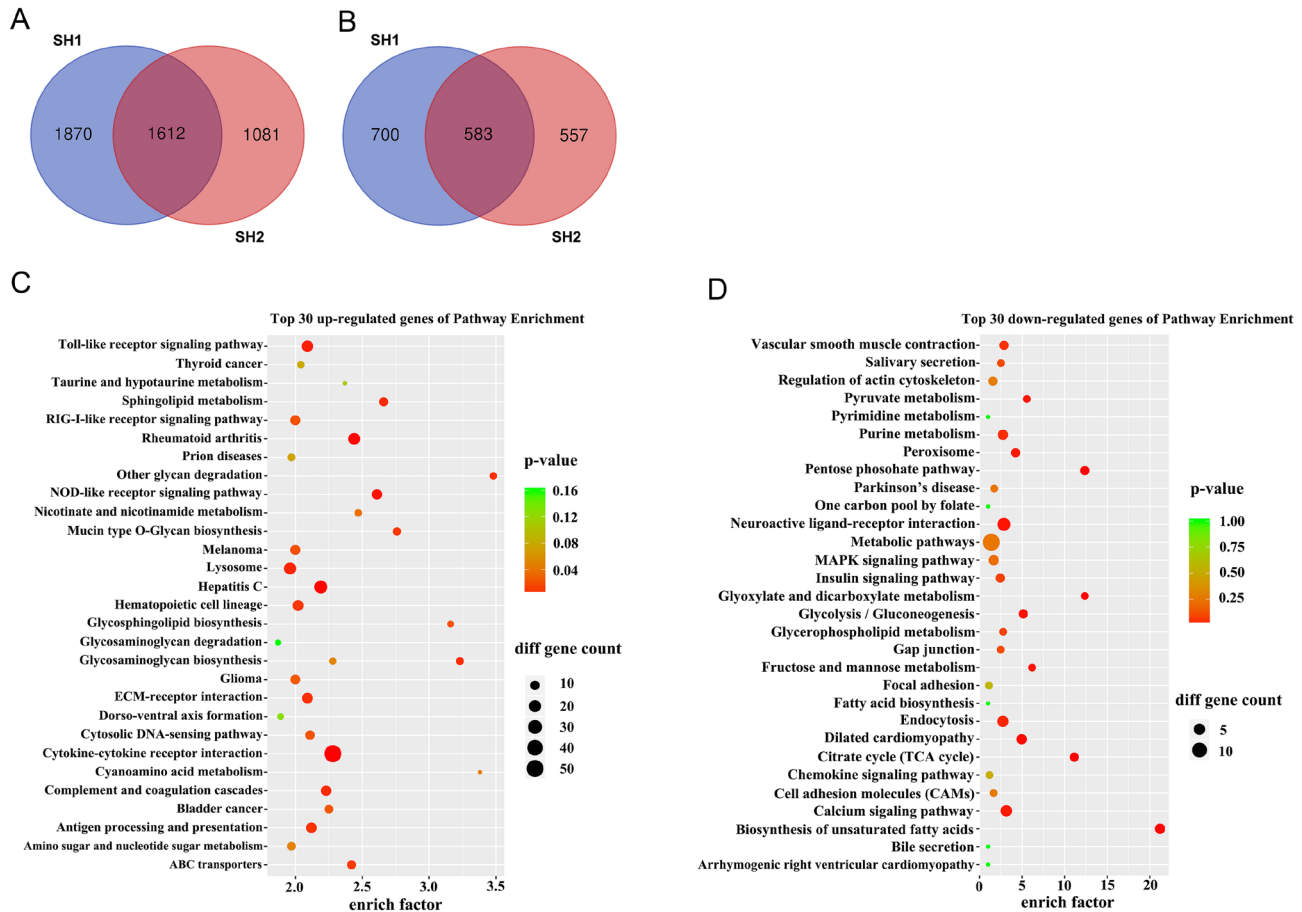
Figure 6
Bioinformatic analysis of differentially expressed mRNAs after RP11 silencing. (A) Intersection analysis showed that 1612 genes were up-regulated in both SH1 and SH2 silence groups when compared with control. (B) Intersection analysis showed that 583 genes were down-regulated in both SH1 and SH2 silence groups. (C) KEGG analysis of top 30 pathways annotations of up-regulated mRNAs may involved in. (D) KEGG analysis of top 30 pathways annotations of down-regulated mRNAs may involved in.

insulin first binds to the tyrosine-autophosphorylated insulin receptor, then activate insulin receptor substrate 1 (IRS1), and finally stimulates glucose transport via activating GLUT-4 (22). Increased insulin levels and GLUT-4 translocation promote glucose uptake and energy storage in the adipose tissue, which inhibits lipolysis and prevents the adipose tissue from supplying energy to other organs (23). In addition, insulin has been shown to stimulate lipid synthesis and suppress lipid degradation through increasing the level of the transcription factor SREBP1c (24). Furthermore, it was shown that IR-deficient (insulin receptors-deficient) mice whose insulin receptors were knocked out displayed lower levels of plasma triglyceride and decreased FM, suggesting that the insulin signaling pathway may promote obesity through regulating glucose and lipid metabolism (25).

The adipose tissue expands by two main mechanisms: hypertrophy or hyperplasia. Obesity is associated with abnormal adipocyte growth, resulting from the induction of preadipocyte differentiation (26). Among the various transcription factors related to adipocyte differentiation, PPARγ is the most critical factor (27). PPARγ, highly expressed in the adipose tissue, has two main isoforms: PPARγ1 and PPARγ2. The former is present in the bulk of the body tissues, while the latter is primarily found in the fat tissue. PPARγ binds another nuclear hormone receptor called retinoid X receptor alpha to form a heterodimer, and regulates the transcription of genes involved in energy and lipid metabolism. Besides, it also activates adipocyte differentiation and promotes fat accumulation. Studies have shown that PPARγ$^{-/-}$ cells may not display adipogenic action due to lack of activation of genes involved in adipogenesis (28, 29). PPARγ signaling is closely linked with the MAPK signaling pathway. Four MAPK cascades have been identified in eukaryotic cells: ERK, Janus tyrosine kinase (JNK)/stress-activated

Endocrine
CONNECTIONS

Y Lin, Y Zhand, L Xu *et al.*

RP11 enhanced preadipocyte
differentiation

10:2

202

Table 3 Top 20 up-regulated and down-regulated mRNAs between RP11 silence and control groups.

Top 20 up-regulated mRNAs				Top 20 down-regulated mRNAs			
SH1/control		SH2/control		SH1/control		SH2/control	
Name	Fold change	Name	Fold change	Name	Fold change	Name	Fold change
RSAD2	162	RSAD2	68.3	RP13-1032I1.10	70.4	FABP7	49.8
CXCL11	104	IFI44L	60.1	GS1-358P8.4	46.3	ACAN	45.8
CXCL10	91.6	SAA1	52.5	HEPACAM	44.3	XXbac-BPG300A18.13	42.2
CMPK2	83.8	MX1	49.2	XXbac-BPG300A18.13	41.0	AC005355.2	34.4
MX1	78.3	CMPK2	48.4	TRIM59	33.9	ULK4P1	27.1
IFI44L	78.0	CXCL10	46.7	LEP	33.3	FAM53B-AS1	26.7
GBP4	74.1	GS1-600G8.5	46.7	ACAN	32.2	FLJ35934	24.5
LGALS9	73.7	C3AR1	45.3	KLHL31	32.0	LEP	24.2
BST2	72.2	HELLPAR	44.3	ADRA2B	31.6	PTGES3L-AARSD1	20.4
CCL5	70.3	BST2	40.8	PTGES3L-AARSD1	31.4	ACTG2	19.9
IFITM1	65.6	TNFSF15	39.7	PNCK	31.1	CXCR4	19.6
IFIT2	63.3	RP11-47I22.2	39.5	CHIA	28.4	YPEL1	19.6
HERC6	61.1	IFITM1	37.9	TRDC	28.4	LRRC31	19.0
USP41	60.4	HERC6	36.6	CA3	27.4	ANGPTL8	18.2
RAB27B	59.4	TFPI2	36.2	ACTG2	26.1	UBE2QL1	18.0
CH25H	59.4	IFI27	35.7	COL11A1	25.8	ADSSL1	17.7
MX2	58.8	OMG	35.1	RP11-80H5.5	24.2	ALDOC	16.7
ISG15	58.1	CXCL11	34.7	GFAP	22.8	RPL32P29	16.7
IFI27	58.1	RP13-143G15.4	33.0	RP11-359E7.3	22.4	PRSS50	16.6
IFIT3	56.7	CH25H	32.4	IGFBPL1	21.8	LRRIQ3	16.5

protein kinase, p38 MAPK, and ERK5 signal transduction pathways (30). Previous evidence suggests that PPARγ can be phosphorylated and regulated by MAPK members, including ERK and p38. The expression and transcription of PPARγ were shown to be increased after ERK and p38 MAPK activation, which promoted the differentiation of adipocytes. Another study conducted by Jung Hwan Oh reported that artemisia princeps suppressed adipocyte differentiation via downregulation of the PPARγ and MAPK pathways (31, 32).

To explore the underlying mechanism of obesity, a previous study focused on the interaction between immune and metabolic systems and proposed a phenomenon called infectobesity (33). Human studies also have shown that intrinsic and proper IFN responses are favorable for antiviral and anti-obesity effects (34). Similarly, the neonates of pregnant women with GDM tend to have more mastadenovirus and papillomavirus in their intestinal flora (35). Mastadenoviruses have been identified as the strongest infectious agents contributing to obesity, and a series of animal studies have confirmed this finding (36). Among the IFN family, type I IFNs, including IFN-α and IFN-β have been largely researched with regards to their role in the immune system and effects on metabolism. A study conducted by Ariel D Quiroga and colleagues demonstrated that IFN-α-2b, belonging to the type I IFN class, exhibits potent anti-obesity effects related to increased fatty acid oxidation and inhibition of the master cholesterogenic transcription factor, SREBP-2, which influences cholesterol

synthesis (37). Kyoungran Lee *et al.* also reported that IFN-α particularly suppresses lipid accumulation during the early phase of adipogenesis. Further, type I IFNs can activate STATs, which have been shown to modulate PPAR-γ signaling through JAK (38). In a previous study, animal experiments showed that IFN-β suppressed inflammatory cell infiltration into adipose tissue as well as production of inflammatory mediators potentially via the inhibition of the nuclear factor kappa B pathway, which subsequently resulted in prevention of adipose hypertrophy and weight gain (39). Additionally, interferon-regulatory factors (IRFs) involved in IFN signaling have also been shown to play a role in the development of adipocytes, and several IRF proteins have been revealed to possess the ability to repress adipogenesis (27). Based on these findings, we speculate that IFNs may play a vital role in the inhibition of adipogenesis, and thus exert anti-obesity effects.

Our study has some limitations. First, we only focus on the expression of RP11 in the umbilical cord blood. Future studies should assess whether the RP11 is differentially expressed after neonatal period, its expression change during the course of pregnancy or it is associated with metabolic controls during pregnancy. Secondly, although we have identified the differentially expressed downstream genes which involved in the adipocyte differentiation, the target gene and the specific mechanism are still unknown. Thirdly, the study were performed in experimental models, additional animal experiments may be needed to confirm our conclusion.

In conclusion, in our study we found that RP11 is highly expressed in the umbilical cord blood of women with GDM macrosomia, and overexpression or silencing of RP11 can significantly promote or inhibit the differentiation of preadipocytes into mature adipocytes, respectively. Furthermore, the differentially expressed downstream genes identified after RP11 silencing may be its target genes, which were found to be closely involved in biological processes related to adipocyte differentiation, such as the insulin signaling pathway, metabolic pathways, MAPK signaling pathway, etc. Although the underlying mechanism and the specific target genes of RP11 remain unclear, our findings can be applied for the future screening of RP11 downstream targets, which will help to further enhance our understanding of GDM-induced fat accumulation.

Supplementary materials

This is linked to the online version of the paper at https://doi.org/10.1530/EC-20-0584.

References

1 American College of Obstetricians and Gynecologists' Committee on Practice Bulletins – Obstetrics. Practice Bulletin No. 173: fetal macrosomia. *Obstetrics and Gynecology* 2016 **128** e195–e209. (https://doi.org/10.1097/AOG.0000000000001767)

2 Koyanagi A, Zhang J, Dagvadorj A, Hirayama F, Shibuya K, Souza JP & Gülmezoglu AM. Macrosomia in 23 developing countries: an analysis of a multicountry, facility-based, cross-sectional survey. *Lancet* 2013 **381** 476–483. (https://doi.org/10.1016/S0140-6736(12)61605-5)

3 Tyrala EE. The infant of the diabetic mother. *Obstetrics and Gynecology Clinics of North America* 1996 **23** 221–241. (https://doi.org/10.1016/s0889-8545(05)70253-9)

4 Anna V, van der Ploeg HP, Cheung NW, Huxley RR & Bauman AE. Sociodemographic correlates of the increasing trend in prevalence of gestational diabetes mellitus in a large population of women between 1995 and 2005. *Diabetes Care* 2008 **31** 2288–2293. (https://doi.org/10.2337/dc08-1038)

5 Filardi T, Catanzaro G, Mardente S, Zicari A, Santangelo C, Lenzi A, Morano S, Ferretti E. Non-coding RNA: role in gestational diabetes pathophysiology and complications. *International Journal of Molecular Sciences* 2020 **21** 4020. (https://doi.org/10.3390/ijms21114020)

6 Sun L, Goff LA, Trapnell C, Alexander R, Lo KA, Hacisuleyman E, Sauvageau M, Tazon-Vega B, Kelley DR, Hendrickson DG, *et al.* Long noncoding RNAs regulate adipogenesis. *PNAS* 2013 **110** 3387–3392. (https://doi.org/10.1073/pnas.1222643110)

7 Alexander R, Lodish H & Sun L. MicroRNAs in adipogenesis and as therapeutic targets for obesity. *Expert Opinion on Therapeutic Targets* 2011 **15** 623–636. (https://doi.org/10.1517/14728222.2011.561317)

8 Guttman M, Donaghey J, Carey BW, Garber M, Grenier JK, Munson G, Young G, Lucas AB, Ach R, Bruhn L, *et al.* lincRNAs act in the circuitry controlling pluripotency and differentiation. *Nature* 2011 **477** 295–300. (https://doi.org/10.1038/nature10398)

9 Gupta RA, Shah N, Wang KC, Kim J, Horlings HM, Wong DJ, Tsai MC, Hung T, Argani P, Rinn JL, *et al.* Long non-coding RNA HOTAIR reprograms chromatin state to promote cancer metastasis. *Nature* 2010 **464** 1071–1076. (https://doi.org/10.1038/nature08975)

10 Klattenhoff CA, Scheuermann JC, Surface LE, Bradley RK, Fields PA, Steinhauser ML, Ding H, Butty VL, Torrey L, Haas S, *et al.* Braveheart, a long noncoding RNA required for cardiovascular lineage commitment. *Cell* 2013 **152** 570–583. (https://doi.org/10.1016/j.cell.2013.01.003)

11 Kretz M, Webster DE, Flockhart RJ, Lee CS, Zehnder A, Lopez-Pajares V, Qu K, Zheng GX, Chow J, Kim GE, *et al.* Suppression of progenitor differentiation requires the long noncoding RNA ANCR. *Genes and Development* 2012 **26** 338–343. (https://doi.org/10.1101/gad.182121.111)

12 Cui X, You L, Li Y, Zhu L, Zhang F, Xie K, Cao Y, Ji C & Guo X. A transcribed ultraconserved noncoding RNA, uc.417, serves as a negative regulator of brown adipose tissue thermogenesis. *FASEB Journal* 2016 **30** 4301–4312. (https://doi.org/10.1096/fj.201600694R)

13 Shi Z, Zhao C, Long W, Ding H & Shen R. Microarray expression profile analysis of long non-coding RNAs in umbilical cord plasma reveals their potential role in gestational diabetes-induced macrosomia. *Cellular Physiology and Biochemistry* 2015 **36** 542–554. (https://doi.org/10.1159/000430119)

14 International Association of Diabetes and Pregnancy Study Groups Consensus Panel, Metzger BE, Gabbe SG, Persson B, Buchanan TA, Catalano PA, Damm P, Dyer AR, Leiva Ad, Hod M, *et al.* International association of diabetes and pregnancy study groups recommendations on the diagnosis and classification of hyperglycemia in pregnancy. *Diabetes Care* 2010 **33** 676–682. (https://doi.org/10.2337/dc09-1848)

15 Tsui NB, Ng EK & Lo YM. Stability of endogenous and added RNA in blood specimens, serum, and plasma. *Clinical Chemistry* 2002 **48** 1647–1653. (https://doi.org/10.1093/clinchem/48.10.1647)

16 Weststrate JA & Deurenberg P. Body composition in children: proposal for a method for calculating body fat percentage from total body density or skinfold-thickness measurements. *American Journal of Clinical Nutrition* 1989 **50** 1104–1115. (https://doi.org/10.1093/ajcn/50.5.1104)

17 Ponting CP, Oliver PL & Reik W. Evolution and functions of long noncoding RNAs. *Cell* 2009 **136** 629–641. (https://doi.org/10.1016/j.cell.2009.02.006)

18 Filardi T, Tavaglione F, Di Stasio M, Fazio V, Lenzi A & Morano S. Impact of risk factors for gestational diabetes (GDM) on pregnancy outcomes in women with GDM. *Journal of Endocrinological Investigation* 2018 **41** 671–676. (https://doi.org/10.1007/s40618-017-0791-y)

19 Basseri S, Lhoták S, Fullerton MD, Palanivel R, Jiang H, Lynn EG, Ford RJ, Maclean KN, Steinberg GR & Austin RC. Loss of TDAG51

results in mature-onset obesity, hepatic steatosis, and insulin resistance by regulating lipogenesis. *Diabetes* 2013 **62** 158–169. (https://doi.org/10.2337/db12-0256)

20 Dahlman I & Arner P. Obesity and polymorphisms in genes regulating human adipose tissue. *International Journal of Obesity* 2007 **31** 1629–1641. (https://doi.org/10.1038/sj.ijo.0803657)

21 Song Z, Xiaoli AM & Yang F. Regulation and metabolic significance of de novo lipogenesis in adipose tissues. *Nutrients* 2018 **10** 1383. (https://doi.org/10.3390/nu10101383)

22 Yazıcı D & Sezer H. Insulin resistance, obesity and lipotoxicity. *Advances in Experimental Medicine and Biology* 2017 **960** 277–304. (https://doi.org/10.1007/978-3-319-48382-5_12)

23 Kubota T, Kubota N & Kadowaki T. Imbalanced insulin actions in obesity and Type 2 diabetes: key mouse models of insulin signaling pathway. *Cell Metabolism* 2017 **25** 797–810. (https://doi.org/10.1016/j.cmet.2017.03.004)

24 Saltiel AR. Insulin signaling in the control of glucose and lipid homeostasis. *Handbook of Experimental Pharmacology* 2016 **233** 51–71. (https://doi.org/10.1007/164_2015_14)

25 Blüher M, Michael MD, Peroni OD, Ueki K, Carter N, Kahn BB & Kahn CR. Adipose tissue selective insulin receptor knockout protects against obesity and obesity-related glucose intolerance. *Developmental Cell* 2002 **3** 25–38. (https://doi.org/10.1016/s1534-5807(02)00199-5)

26 Ghaben AL & Scherer PE. Adipogenesis and metabolic health. *Nature Reviews: Molecular Cell Biology* 2019 **20** 242–258. (https://doi.org/10.1038/s41580-018-0093-z)

27 Mota de Sá P, Richard AJ, Hang H & Stephens JM. Transcriptional regulation of adipogenesis. *Comprehensive Physiology* 2017 **7** 635–674. (https://doi.org/10.1002/cphy.c160022)

28 Rosen ED, Hsu CH, Wang X, Sakai S, Freeman MW, Gonzalez FJ & Spiegelman BM. C/EBPalpha induces adipogenesis through PPARgamma: a unified pathway. *Genes and Development* 2002 **16** 22–26. (https://doi.org/10.1101/gad.948702)

29 He W, Barak Y, Hevener A, Olson P, Liao D, Le J, Nelson M, Ong E, Olefsky JM & Evans RM. Adipose-specific peroxisome proliferator-activated receptor gamma knockout causes insulin resistance in fat and liver but not in muscle. *PNAS* 2003 **100** 15712–15717. (https://doi.org/10.1073/pnas.2536828100)

30 Guo YJ, Pan WW, Liu SB, Shen ZF, Xu Y & Hu LL. ERK/MAPK signalling pathway and tumorigenesis. *Experimental and Therapeutic Medicine* 2020 **19** 1997–2007. (https://doi.org/10.3892/etm.2020.8454)

31 Haridas Nidhina PA, Poulose N & Gopalakrishnapillai A. Vanillin induces adipocyte differentiation in 3T3-L1 cells by activating extracellular signal regulated kinase 42/44. *Life Sciences* 2011 **88** 675–680. (https://doi.org/10.1016/j.lfs.2011.02.001)

32 Oh JH, Karadeniz F, Lee JI, Seo Y & Kong CS. Artemisia princeps inhibits adipogenic differentiation of 3T3-L1 pre-adipocytes via downregulation of PPARγ and MAPK pathways. *Preventive Nutrition and Food Science* 2019 **24** 299–307. (https://doi.org/10.3746/pnf.2019.24.3.299)

33 Pasarica M & Dhurandhar NV. Infectobesity: obesity of infectious origin. *Advances in Food and Nutrition Research* 2007 **52** 61–102. (https://doi.org/10.1016/S1043-4526(06)52002-9)

34 Tian Y, Jennings J, Gong Y & Sang Y. Viral infections and interferons in the development of obesity. *Biomolecules* 2019 **9** 726. (https://doi.org/10.3390/biom9110726)

35 Wang J, Zheng J, Shi W, Du N, Xu X, Zhang Y, Ji P, Zhang F, Jia Z, Wang Y, *et al.* Dysbiosis of maternal and neonatal microbiota associated with gestational diabetes mellitus. *Gut* 2018 **67** 1614–1625. (https://doi.org/10.1136/gutjnl-2018-315988)

36 Huo L, Lyons J & Magliano DJ. Infectious and environmental influences on the obesity epidemic. *Current Obesity Reports* 2016 **5** 375–382. (https://doi.org/10.1007/s13679-016-0224-9)

37 Quiroga AD, Comanzo CG, Heit Barbini FJ, Lucci A, Vera MC, Lorenzetti F, Ferretti AC, Ceballos MP, Alvarez ML & Carrillo MC. IFN-α-2b treatment protects against diet-induced obesity and alleviates non-alcoholic fatty liver disease in mice. *Toxicology and Applied Pharmacology* 2019 **379** 114650. (https://doi.org/10.1016/j.taap.2019.114650)

38 Lee K, Um SH, Rhee DK & Pyo S. Interferon-alpha inhibits adipogenesis via regulation of JAK/STAT1 signaling. *Biochimica et Biophysica Acta* 2016 **1860** 2416–2427. (https://doi.org/10.1016/j.bbagen.2016.07.009)

39 Alsaggar M, Mills M & Liu D. Interferon beta overexpression attenuates adipose tissue inflammation and high-fat diet-induced obesity and maintains glucose homeostasis. *Gene Therapy* 2017 **24** 60–66. (https://doi.org/10.1038/gt.2016.76)